Collinear generation of ultrashort UV and XUV pulses

E. M. Bothschafter[1,2], A. Schiffrin[1], V.S. Yakovlev[1,3], A.M. Azzeer[4], F. Krausz[1,3], R. Ernstorfer[2,*] and R. Kienberger[1,2]

[1] *Max-Planck-Institut für Quantenoptik, Hans-Kopfermann-Str. 1, D-85748 Garching, Germany.*
[2] *Physik-Department E11, Technische Universität München, James Franck Str., D-85748 Garching, Germany.*
[3] *Department für Physik, Ludwig-Maximilians-Universität, Am Coulombwall 1, D-85748 Garching, Germany.*
[4] *Department of Physics and Astronomy, King Saud University, P.O. Box 2455, Riyadh 11451, Kingdom of Saudi Arabia.*
* ralph.ernstorfer@mpq.mpg.de

Abstract: We demonstrate the collinear generation of few-femtosecond ultraviolet and attosecond extreme ultraviolet pulses via a combination of third-harmonic and high harmonic generation in noble gases. The ultrashort coherent light bursts are produced by focusing a sub-1.5-cycle near-infrared/visible laser pulse in two subsequent quasi-static noble gas targets. This approach provides an inherently synchronized pair of UV and XUV pulses, where the UV radiation has a photon energy of ~5 eV and a pulse energy of up to 1 μJ and the XUV radiation contains up to $3.5 \cdot 10^6$ XUV photons per shot with a photon energy exceeding 100 eV. This source represents a novel tool for future UV pump/XUV probe experiments with unprecedented time-resolution.

© 2010 Optical Society of America

OCIS codes: (190.7110) Ultrafast nonlinear optics; (190.7220) Upconversion, (190.4180) Multiharmonic generation, (260.7190) Ultraviolet, (260.7200) Ultraviolet, extreme

---

References and links

1. M. Uiberacker, T. Uphues, M. Schultze, A. J. Verhoef, V. Yakovlev, M. F. Kling, J. Rauschenberger, N. M. Kabachnik, H. Schröder, M. Lezius, K. L. Kompa, H. G. Muller, M. J. J. Vrakking, S. Hendel, U. Kleineberg, U. Heinzmann, M. Drescher, and F. Krausz, "Attosecond real-time observation of electron tunnelling in atoms," Nature **446**(7136), 627–632 (2007).
2. P. Eckle, M. Smolarski, P. Schlup, J. Biegert, A. Staudte, M. Schoffler, H. G. Muller, R. Dorner, and U. Keller, "Attosecond angular streaking," Nat. Phys. **4**(7), 565–570 (2008).
3. A. L. Cavalieri, N. Müller, T. Uphues, V. S. Yakovlev, A. Baltuska, B. Horvath, B. Schmidt, L. Blümel, R. Holzwarth, S. Hendel, M. Drescher, U. Kleineberg, P. M. Echenique, R. Kienberger, F. Krausz, and U. Heinzmann, "Attosecond spectroscopy in condensed matter," Nature **449**(7165), 1029–1032 (2007).
4. R. Kienberger, E. Goulielmakis, M. Uiberacker, A. Baltuska, V. Yakovlev, F. Bammer, A. Scrinzi, T. Westerwalbesloh, U. Kleineberg, U. Heinzmann, M. Drescher, and F. Krausz, "Atomic transient recorder," Nature **427**(6977), 817–821 (2004).
5. M. Hentschel, R. Kienberger, C. Spielmann, G. A. Reider, N. Milosevic, T. Brabec, P. Corkum, U. Heinzmann, M. Drescher, and F. Krausz, "Attosecond metrology," Nature **414**(6863), 509–513 (2001).
6. J. Itatani, F. Quéré, G. L. Yudin, M. Y. Ivanov, F. Krausz, and P. B. Corkum, "Attosecond streak camera," Phys. Rev. Lett. **88**(17), 173903 (2002).
7. P. S. Kirchmann, P. A. Loukakos, U. Bovensiepen, and M. Wolf, "Ultrafast electron dynamics studied with time-resolved two-photon photoemission: intra- and interband scattering in C6F6/Cu(111)," N. J. Phys. **7**, 113 (2005).
8. M. Bauer, "Femtosecond ultraviolet photoelectron spectroscopy of ultra-fast surface processes," J. Phys. D Appl. Phys. **38**(16), R253–R267 (2005).
9. G. Saathoff, L. Miaja-Avila, M. Aeschlimann, M. M. Murnane, and H. C. Kapteyn, "Laser-assisted photoemission from surfaces," Phys. Rev. A **77**(2), 022903 (2008).
10. P. Baum, S. Lochbrunner, and E. Riedle, "Tunable sub-10-fs ultraviolet pulses generated by achromatic frequency doubling," Opt. Lett. **29**(14), 1686–1688 (2004).
11. N. Aközbek, A. Iwasaki, A. Becker, M. Scalora, S. L. Chin, and C. M. Bowden, "Third-harmonic generation and self-channeling in air using high-power femtosecond laser pulses," Phys. Rev. Lett. **89**(14), 143901 (2002).
12. C. G. Durfee 3rd, S. Backus, H. C. Kapteyn, and M. M. Murnane, "Intense 8-fs pulse generation in the deep ultraviolet," Opt. Lett. **24**(10), 697–699 (1999).
13. T. Fuji, T. Horio, and T. Suzuki, "Generation of 12 fs deep-ultraviolet pulses by four-wave mixing through filamentation in neon gas," Opt. Lett. **32**(17), 2481–2483 (2007).

14. K. Kosma, S. A. Trushin, W. E. Schmid, and W. Fuß, "Vacuum ultraviolet pulses of 11 fs from fifth-harmonic generation of a Ti:sapphire laser," Opt. Lett. **33**(7), 723–725 (2008).
15. U. Graf, M. Fiess, M. Schultze, R. Kienberger, F. Krausz, and E. Goulielmakis, "Intense few-cycle light pulses in the deep ultraviolet," Opt. Express **16**(23), 18956–18963 (2008).
16. J. J. Macklin, J. D. Kmetec, and C. L. Gordon 3rd, "High-order harmonic generation using intense femtosecond pulses," Phys. Rev. Lett. **70**(6), 766–769 (1993).
17. A. L'Huillier, and P. Balcou, "High-Order Harmonic Generation in Rare Gases with a 1-Ps 1053-Nm Laser," Phys. Rev. Lett. **70**(6), 774–777 (1993).
18. P. B. Corkum, "Plasma Perspective on Strong Field Multiphoton Ionization," Phys. Rev. Lett. **71**(13), 1994–1997 (1993).
19. F. Brunel, "Harmonic-Generation Due to Plasma Effects in a Gas Undergoing Multiphoton Ionization in the High-Intensity Limit," J. Opt. Soc. Am. B **7**(4), 521–526 (1990).
20. A. L. Cavalieri, E. Goulielmakis, B. Horvath, W. Helml, M. Schultze, M. Fiess, V. Pervak, L. Veisz, V. S. Yakovlev, M. Uiberacker, A. Apolonski, F. Krausz, and R. Kienberger, "Intense 1.5-cycle near infrared laser waveforms and their use for the generation of ultra-broadband soft-x-ray harmonic continua," N. J. Phys. **9**(7), 242 (2007).
21. E. Goulielmakis, M. Schultze, M. Hofstetter, V. S. Yakovlev, J. Gagnon, M. Uiberacker, A. L. Aquila, E. M. Gullikson, D. T. Attwood, R. Kienberger, F. Krausz, and U. Kleineberg, "Single-cycle nonlinear optics," Science **320**(5883), 1614–1617 (2008).
22. M. Nisoli, E. Priori, G. Sansone, S. Stagira, G. Cerullo, S. De Silvestri, C. Altucci, R. Bruzzese, C. de Lisio, P. Villoresi, L. Poletto, M. Pascolini, and G. Tondello, "High-brightness high-order harmonic generation by truncated bessel beams in the sub-10-fs regime," Phys. Rev. Lett. **88**(3), 033902 (2002).
23. P. Salieres, T. Ditmire, K. S. Budil, M. D. Perry, and A. L'Huillier, "Spatial Profiles of High-Order Harmonics Generated by a Femtosecond Crlisaf Laser," J. Phys. At. Mol. Opt. Phys. **27**(9), L217–L222 (1994).
24. T. Bartel, P. Gaal, K. Reimann, M. Woerner, and T. Elsaesser, "Generation of single-cycle THz transients with high electric-field amplitudes," Opt. Lett. **30**(20), 2805–2807 (2005).
25. Y. Chen, M. Yamaguchi, M. Wang, and X.-C. Zhang, "Terahertz pulse generation from noble gases," Appl. Phys. Lett. **91**(25), 251116 (2007).
26. M. Kreß, T. Löffler, M. D. Thomson, R. Dörner, H. Gimpel, K. Zrost, T. Ergler, R. Moshammer, J. Ullrich, and H. G. Roskos, "Determination of the carrier-envelope phase of few-cycle laser pulses with terahertz-emission spectroscopy," Nat. Phys. **2**(5), 327–331 (2006).
27. IRD, "International Radiation Detectors," *http://www.ird-inc.com/axuvwdd/axuv-100_zr_c.htm*.
28. D. L. Windt, "IMD - Software for modeling the optical properties of multilayer films," Comput. Phys. **12**(4), 360–370 (1998).
29. F. J. Himpsel, P. Heimann, T. C. Chiang, and D. E. Eastman, "Geometry-Dependent Si(2p) Surface Core-Level Excitations for Si(111) and Si(100) Surfaces," Phys. Rev. Lett. **45**(13), 1112–1115 (1980).
30. A. Bideaumehu, Y. Guern, R. Abjean, and A. Johanningilles, "Measurement of refractive-indexes of neon, Argon, krypton and xenon in the 253.7-140.4 nm wavelength range - Dispersion-relations and estimated oscillator-strengths of the resonance lines," J. Quant. Spectrosc. Radiat. Transf. **25**(5), 395–402 (1981).
31. V. Tosa, H. T. Kim, I. J. Kim, and C. H. Nam, "High-order harmonic generation by chirped and self-guided femtosecond laser pulses. I. Spatial and spectral analysis," Phys. Rev. A **71**(6), 063807 (2005).
32. M. Mlejnek, E. M. Wright, and J. V. Moloney, "Femtosecond pulse propagation in argon: A pressure dependence study," Phys. Rev. E Stat. Phys. Plasmas Fluids Relat. Interdiscip. Topics **58**(4), 4903–4910 (1998).

1. Introduction

Within the last decade attosecond metrology has been established as a tool for studying some of the fastest processes in nature, for example, field-induced tunneling of electrons in atoms [1, 2] and electron transport in solids on sub-nm length scales [3]. One spectroscopic technique for accessing this time domain is the attosecond transient recorder (ATR) [4]. This method is based on the availability of isolated attosecond (1 as $=10^{-18}$ s) pulses in the extreme ultraviolet (XUV) that are synchronized to a carrier envelope phase-stabilized few-cycle near-infrared (NIR) laser pulse. The momentum of photoelectrons emitted by the attosecond XUV pulse is altered depending on the strength of the vector potential at the time when the electron is released [5, 6]. Based on this concept, the ATR is a technique for studying the time of photoemission of electrons originating from ground states. In order to investigate the dynamics of excited electronic wave-packets, for instance, resolving the formation and relaxation of photo-excited electrons in valence states of atoms, molecules or solids on the attosecond to few-femtosecond timescale, it is highly desirable to generate an intense femtosecond light pulse in the ultraviolet (UV) spectral range in addition to an attosecond XUV pulse. Employing the conventional pump-probe scheme of time-resolved two-photon photoemission spectroscopy (TR-2PPE) [7–9], ultraviolet light-induced transient electron populations are photoemitted by the subsequent synchronized XUV pulse at well-defined time

delays. With the availability of isolated attosecond XUV pulses, this UV-XUV TR-2PPE scheme offers the intriguing possibility to study excited state dynamics with a time-resolution shorter than the optical period of the pump pulse

Our work aims to provide the prerequisites, i.e., highly synchronized UV and XUV pulses with the required pulse duration for this type of experiments. Since no suitable broadband laser material is available in the ultraviolet domain, the generation of ultrashort UV laser pulses relies on nonlinear frequency mixing and frequency up-conversion of femtosecond laser pulses in solids [10] and gases [11–15]. When multi-cycle laser pulses are used for generation [10–14], pulse durations below 10 fs can only be reached by compressing the generated UV pulses and precisely controlling and tuning the dispersion in the ultraviolet after the generation process. Recently, it has been demonstrated that third-harmonic generation from Fourier-limited few-cycle NIR laser pulses in noble gases directly provides intense sub-4 fs pulses in the deep ultraviolet spectral range [15]. While this process relies on the induced polarization due to the third-order electric susceptibility $\chi^{(3)}$ of the gas and therefore is favored in high-density media, higher-order harmonics can be generated with a very similar technique in low-density gases in a different regime [16, 17]. High harmonic generation can be described in a semi-classical three-step model [18, 19] involving tunnel ionization of the least bound electron of a noble gas atom [19], acceleration of the electron in the electric field followed by recombination with the atomic core, upon which the electron emits its excess energy in a short, high energetic burst of light. This process is triggered and completed every half-cycle of the driving laser field, so that by using NIR light pulses approaching the single-oscillation limit [20] the photons with the highest energy are emitted during a single half cycle. Filtering these so-called high-harmonic cut-off photons yields isolated XUV pulses with pulse durations below 100 as [21].

In the following we present a novel approach for generating ultrashort UV and attosecond XUV pulses that are inherently synchronized using a collinear configuration of two quasi-static gas cells in a single laser focus.

2. Experimental setup

The vacuum chamber employed in this work is shown schematically in Fig. 1. Two static gas cells (nickel tube, 2-3 mm diameter, 0.1 mm wall thickness) are placed in the focus (f=600 mm) of a few-cycle NIR laser beam. Both targets can be independently supplied with arbitrary gases and pressures exceeding 10 bar. In practice, the first gas target is optimized for third-harmonic generation and therefore it is supplied with several bar of either argon (Ar) or neon (Ne). The second gas target is typically supplied with several hundreds of mbar of Ne with the exact pressure being optimized for high harmonic generation. The holes in the targets through which the laser beam and the generated harmonics propagate are drilled by the focused fundamental laser beam and have a diameter of ~100 μm.

The gas load emerging from the gas targets is pumped differentially by using a second vacuum chamber nested inside the main vacuum setup with two small apertures (Ø 0.7 mm) for the laser beams and a total width of 50 mm in direction of propagation of the laser beam. This measure minimizes absorption and group velocity dispersion of the generated UV and XUV pulses after their generation. The two gas targets are placed inside of this small chamber and therefore the propagation distances of the fundamental laser beam and of the generated harmonic radiation in the region with a background pressure of 10^{-2}–1 mbar are approximately 50 mm and 25 mm, respectively. The gas target pressures given in the experimental section apply to the backing pressure of the gas targets. The fact that the background pressure is at least two orders of magnitude smaller than the backing pressure assures that the interaction region of the laser is mostly confined to the width of the gas targets.

Both targets can be positioned independently inside this small chamber in all three dimensions for alignment. The positions of the gas targets in direction of the laser beam (x_1, x_2 in Fig. 1) with respect to the laser focus and to each other are optimized for collinear generation. The optimal distance between x_1 and x_2 is typically a few millimeters and changes

in dependence of the gas pressure applied to the UV target as this affects the fundamental laser field as discussed below in section 3.3.

The parameters of the NIR laser pulses are similar to those in [20]. The nearly Fourier-limited sub-4 fs 400 μJ pulses have a 450 nm broad spectrum centered at 720 nm. The focusing geometry corresponds to the one used for the generation of isolated attosecond pulses. The peak intensity in the focus can be tuned with an iris in front of the focusing mirror and its maximum is $7 \cdot 10^{14}$ W/cm^2.
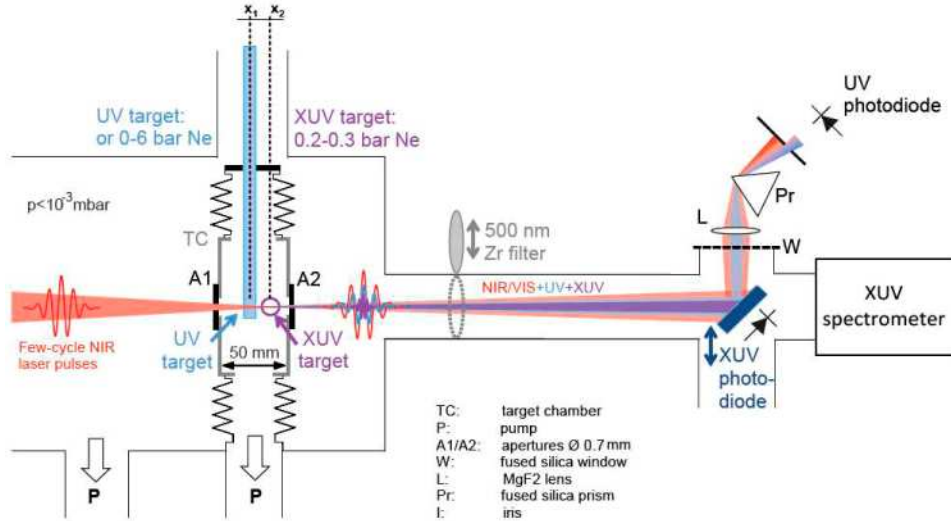
Fig. 1. Collinear generation of UV and XUV pulses in two subsequent gas targets. The targets, formed by 2 to 3 mm thick nickel tubes, can be positioned independently (x1, x2). They are situated inside a main vacuum setup in a small, differentially pumped vacuum chamber with two apertures (Ø 0.7 mm) for the laser. The few-cycle 720 nm NIR pulses (sub-4 fs, 400 μJ) are focused into the XUV gas target (purple) which is supplied with 0.2 - 0.3 bar Ne. The UV target (blue) is placed in front of the XUV target and supplied with Ar or Ne at variable pressure. The number of XUV photons per pulse is measured with an XUV diode placed under 45° in the beam path of the co-propagating NIR, UV and XUV beams. The diode is coated with a filter layer that partially reflects the NIR and the UV through a fused silica window outside the vacuum system, where the UV can be characterized in spectrum and pulse energy after separation from the IR with a prism. For the measurement of the XUV an additional 500 nm zirconium filter is inserted in front of the diode. The diode can be retracted for spectral characterization of the XUV with a grazing incidence grating (600 l/mm) spectrometer.

Behind the gas targets, the NIR, the UV and the XUV laser pulses propagate collinearly with different divergence depending on the respective wavelength [22, 23]. According to recent reports of THz generation from gases driven by femtosecond laser pulses [24–26], we also expect high field amplitude THz emission from the gas targets. This would add yet another source of ultrashort pulses in a different spectral range and will be subject of further investigations.

The number of XUV photons per pulse is measured with an XUV diode (International Radiation Detectors, AXUV100) placed under an angle of 45° in the co-propagating NIR, UV and XUV beams. The diode is coated with a directly deposited filter consisting of 200 nm zirconium (Zr), 10 nm amorphous carbon (a-C), 100 nm molybdenum (Mo) and 5 nm boron carbide (B$_4$C). In addition to that, a 500 nm Zr filter was inserted perpendicularly to the propagation direction to block the fundamental laser completely.

The quantum efficiency of the diode with a 200 nm Zr and 50 nm a-C is specified by the manufacturer [27] and shown as dashed curve in Fig. 2. The transmission of the various filter layers in the setup under the respective angle of incidence is calculated with IMD [28]. A correction for the reduced transmission through the custom filter layers of the specified

quantum efficiency gives the effective quantum efficiency of the diode, shown as solid line in Fig. 2. The average quantum efficiency of 0.45 in the spectral window between 6.5 nm and 13.5 nm was used to calculate the absolute value of XUV photons per pulse from the amplified diode signal.

The change in transmission of the filter layer between normal and 45° incidence was also evaluated experimentally and shows a significantly stronger attenuation under 45° incidence than the calculations predict. Therefore our results represent a conservative measure of the number of XUV photons per pulse in the transmission window of the filter layers.
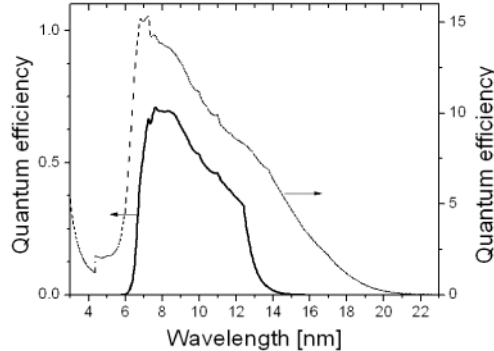
Fig. 2. XUV diode effective quantum efficiency (solid line) calculated from the quantum efficiency specified for the diode with a 200 nm Zr/ 50 nm C coating by manufacturer (dashed line) with corrections for custom filter layer.

The XUV spectra are measured with a grazing incidence grating (600 lines/mm) spectrometer (McPherson, 248/100G). The energy axes of the spectra are calibrated using the L-absorption edge of silicon at ~100 eV [29] by comparing spectra transmitted through a 200 nm thick silicon filter with the simulated transmission curve [28].

The filter layer on the XUV diode partially reflects the NIR and the UV outside the vacuum system through a fused silica window, where the UV is separated from the NIR with a prism and an aperture after recollimation with a lens. The UV pulse energy is measured with a low energy photodiode head (Ophir Optronics Ldt., PD10) with reflection losses on the diode, the window, the prism and the lens being taken into account. For the spectral characterization of the UV pulses with a VIS/UV spectrometer (Maya Pro 2000, 220 - 1100 nm, Ocean Optics), the NIR radiation is suppressed by two reflections at a Si wafer surface under Brewster's angle for 720 nm. As described in [15], this method suppresses the NIR up to two orders of magnitude of the NIR laser. The UV spectra have been corrected for the spectral modification induced by two reflections on silicon.

3. Experimental results

We characterized the influence of the UV gas target on the XUV generation in order to evaluate the suitability of collinear generation for ultrafast UV pump/XUV probe experiments.

3.1 Measurement of the UV pulse energy and number of XUV photons per pulse

The UV pulse energy was measured in dependence of the gas pressure in the UV target for Ar and Ne; the results are plotted as full squares in Figs. 3(a) and 3(b), respectively. The conversion efficiency of the NIR to the third harmonic can be tuned with the UV target pressure and we can achieve UV pulses with energies up to 1 μJ, which is in good agreement with previous results [15]. The number of photons per XUV pulse, collinearly generated in the second target filled with 270 mbar Ne is shown in Fig. 3(a) and (b) as circles. Without any gas being applied in the UV target, the high harmonic generation provides up to $3.5 \cdot 10^6$ photons per pulse corresponding to a pulse energy exceeding 50 pJ. The Ne pressure in the XUV target was optimized for XUV generation and kept constant at 270 mbar. For Ne being

used in the UV target, the XUV signal (Fig. 3(b), circles) decreases almost linearly when the pressure in the UV target is increased to 1.5 bar. For further increasing pressure, the slope of the curve gets smaller. When Ar is used in the UV target, a quantitatively comparable but much steeper decrease with increasing pressure is observed. This is followed by an almost constant XUV signal for pressures above 600 mbar.

We find that the UV pulse energy can be tuned over a several hundred nJ range and still 10^6 photons per pulse with photon energies exceeding 100 eV can be achieved in co-propagating XUV pulses that are synchronized with the UV pulses.
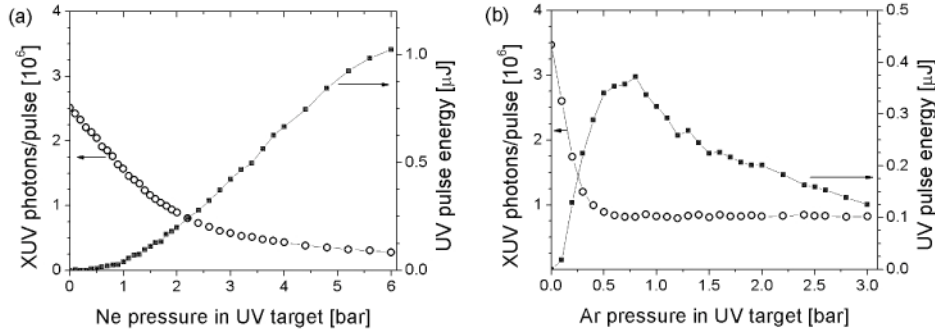
Fig. 3. XUV photon number per pulse (circles) and UV pulse energy (full squares) as functions of the gas pressure in the UV target for Ne (a) and Ar (b). The Ne pressure in the XUV target was kept constant at 270 mbar.

3.2 Spectral characterization

The spectral characterization of the UV and XUV pulses under identical conditions during collinear generation is shown in Fig. 4 and Fig. 5. The spectrum of the UV light generated in Ne (Fig. 4(a)) shows no dependence on the UV target pressure. The spectra from the bottom to the top correspond to the UV pulse energies of 30%, 65% and 100% of the maximal achievable value in Ne. The spectrum of Ar-generated UV pulses narrows with increasing pressure (Fig. 4(b)). This can be attributed to a loss in phase matching bandwidth that also affects the conversion efficiency at higher Ar pressures.

The normalized spectra of the third harmonic (UV) have been corrected for two reflections on Si wafers under Brewster's angle for 720 nm. The spectra are centered at approximately 5 eV and range from 4.5 eV to more than 5.5 eV. On the high energy side, the spectral characterization is restricted by the sensitivity range of the spectrometer.
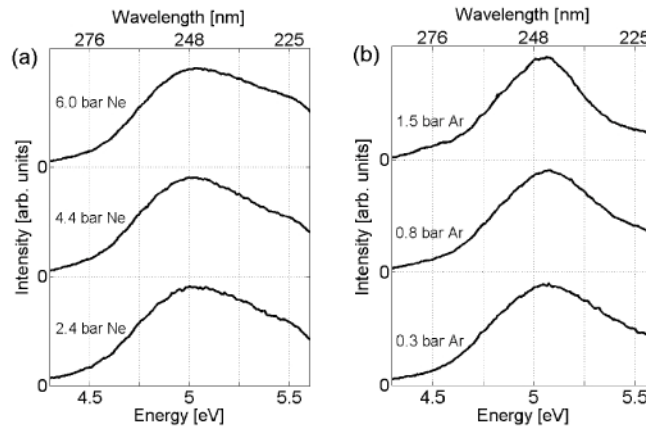

Fig. 4. UV spectra after both gas targets. The XUV radiation was generated in 270 mbar Ne and the UV was generated in Ne (a) and Ar (b) at the respective pressures given in the figure.

In order to estimate the temporal spread of the UV pulses due to propagation through the XUV gas target, we calculated the group velocity dispersion of Ne at 1 bar according to the Sellmeier formula taken from [30] to be 0.06·fs^2/mm at 245 nm. As the XUV target is only 3 mm thick and the pressure in the target is around 300 mbar, we expect that the UV pulse duration is comparable to the results achieved previously with this technique [15]. For instance, the full-width half-maximum bandwidth of the spectrum generated in 6 bar Ne supports pulse durations down to 2.3 fs for a Fourier-limited pulse.

The normalized XUV spectra show in both cases that the cut-off is shifted towards lower photon energies as the pressure in the UV target is increased. This red-shift of the high harmonic cut-off occurs both when Ar or Ne is being used in the UV target.
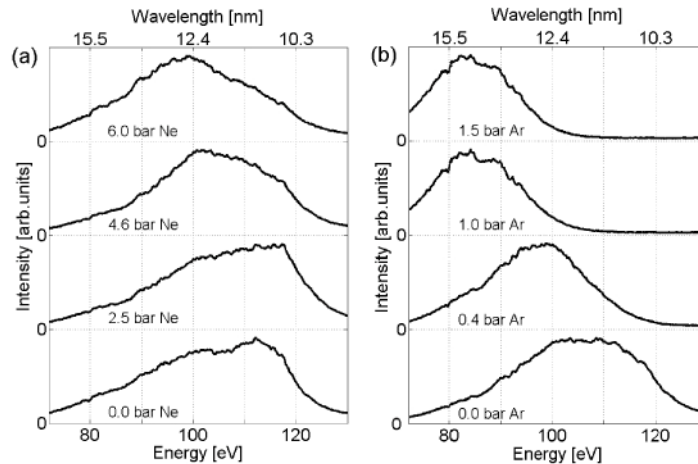

Fig. 5. XUV spectra generated in 230 mbar Ne. In the first gas jet, UV was generated simultaneously in Ne (a) or Ar (b) at the respective pressures given in the figures. (a) The detector strongly attenuates spectra above 115 eV, so that the cut-off of the spectrum lies outside of the detector's range for the spectra at 0 bar and 2.5 bar. With rising pressure in the UV target, the cut-off shifts toward lower energies with rising Ne pressure (bottom to top) in the UV target. (b) When Ar is being used for UV generation, the XUV cut-off also shifts toward lower energies when the pressure rises from 0 to 1 bar but remains constant for higher pressures.

3.3 Interpretation of the results

Qualitatively, the red shift of the XUV cut-off and the decrease of the XUV signal in dependence of the pressure and the gas in the UV target can be explained by changes of the fundamental laser pulse properties such as pulse shape, instantaneous frequency and peak intensity. These are mainly caused by intensity-dependent ionization of the gas in the UV target. Assuming a radial intensity profile with its peak at the center, the negative free-electron dispersion in the resulting plasma is initially non-uniform in the plane of the pulse front. The free-electron density is higher on the axis of the laser propagation and decreases radially. Therefore, the ionized gas acts like a defocusing lens and changes the radius of curvature of the converging laser beam [31, 32] which eventually results in a flat-top-like intensity profile. Once this is reached, the ionization probability becomes uniform over the central part of the beam and the laser pulse propagates in a self-guided fashion.

Due to the difference in ionization potential between Ar and Ne, the ionization probability at low pressures is higher for Ar than it is for Ne at the same laser intensity. The XUV signal measured in dependence of the pressure in the UV target gives an indication that the laser pulse propagating through the UV target reaches the stable flat-top-like profile already at pressures around 0.5 bar in Ar whereas in Ne this is only approached at pressures above 5 bar. The red-shift of the XUV cut-off is also in good agreement with this interpretation, as highest achievable photon energy depends linearly on the laser intensity [18].

In addition to the defocusing of the NIR beam, we also expect a contribution to the red-shift of the XUV cut-off energy resulting from a dynamic blue-shift of the instantaneous frequency of the NIR pulse [5] during propagation through the ionized gas in the UV target.

4. Conclusions

We have successfully demonstrated the collinear generation of UV and XUV pulses by means of third-harmonic generation and high-order harmonic generation in a noble gas with a quasi single-cycle NIR laser pulse. While simultaneously providing XUV pulses with up to 3.5 10^6 photons per pulse and a cut-off photon energy of more than 100 eV, our approach allows obtaining UV pulses with a pulse energy tunable up to ~1 μJ generated in either Ne or Ar by varying the gas target pressure. The shape of the UV spectra, centered at ~5 eV, was shown to be preserved as the gas pressure was varied. As we are able to minimize the dispersion of the generated harmonic radiation due to background noble gas pressure, the collinearly generated UV and XUV pulses are expected to have a temporal structure comparable to the ones produced independently and reported in previous studies [15,21], with respective durations in the sub-4 fs and attosecond timescales. The presented method of collinear generation provides an inherent synchronization between the UV and the XUV pulses. Such findings represent a novel real-time optical tool providing a few-fs time resolution with which the dynamics of excited electronic states in atomic, molecular and condensed matter systems exhibiting absorption resonances in the UV or XUV can be addressed.

Acknowledgements